NANO LETTERS

2006
Vol. 6, No. 6
1240−1244

Measurement of Current-Induced Local Heating in a Single Molecule Junction

Zhifeng Huang,[†] Bingqian Xu,[†] Yuchang Chen,[§] Massimiliano Di Ventra,*[,‡] and Nongjian Tao*[,†]

Department of Electrical Engineering & The Center for Solid State Electronics Research, Arizona State University, Tempe, Arizona 85287, Department of Physics, University of California, San Diego, La Jolla, California 92093, and Department of Electrophysics, National Chiao Tung University, Hsinchu 30010, Taiwan

Received April 12, 2006

ABSTRACT

We have studied the current-induced local heating effects in single molecules covalently bound to two electrodes by measuring the force required to break the molecule–electrode bonds under various conditions. The breakdown process is thermally activated, which is used to extract the effective temperature of the molecular junction as a function of applied bias voltage. We have also performed first-principles calculations of both local heating and current-induced force effects, and the results are in good agreement with the experimental findings.

Understanding electron transport through a single molecule attached to two electrodes is a basic task in molecular electronics.[1−3] Because local heating is known to be an important factor in the design of conventional silicon-based microelectronics, it is natural to ask how important this effect is in such electrode−molecule−electrode structures. Local heating arises from energy exchanged between electrons and phonons.[4,5] In a nanoscale junction, the inelastic electron mean free path is often large compared to the size of the junction so that each electron, on average, is expected to release only a small amount of its energy during transport in the junction. However, substantial local heating can still arise because of the large current density, and thus power per atom, in the nanojunction compared to the bulk. Recently, experimental studies of local heating effects in atomic scale metal contacts have been reported.[6,7] In the case of molecules, the current density is usually much lower than in metallic quantum point contacts but the thermal conduction of molecules is also expected to be poorer than the metal contacts. Several theoretical calculations have found a finite increase in the temperature of the molecules as a result of inelastic scattering of electrons.[5,8,9] However, measurement of current-induced local heating in a single molecule has not been carried out because of the lack of a suitable experimental method.

Here we report on an experimental approach to determine the local temperature in a single molecule covalently bound to two gold electrodes. We measure the force required to break down the attachment of the molecules to the electrodes using a modified conducting atomic force microscopy (C-AFM) (Figure 1a). Because the breakdown process is thermally activated, the average breakdown force is sensitive to the local temperature of the molecule−electrode contact, which allows us to estimate the effective local temperature of the molecular junction. We have also performed first-principles calculations of the local temperature and current-induced forces on the same molecule, and found good agreement with the experimental findings.

We chose octanedithiol as a model system for studying local heating effects because of the following reasons. First, the molecule is terminated with thiol groups on both ends so that they can covalently bind to two Au electrodes simultaneously. Second, it has a rather large HOMO−LUMO gap and its conduction mechanism is due to electron tunneling.[10−16] Finally, this molecule has been widely studied by various techniques.[10−17] We have determined the conductance of octanedithiol recently by repeatedly creating gold−molecule−gold junctions using a STM-break junction approach.[16,18,19] The conductance histogram constructed from the repeated measurements reveals two sets of well-defined peaks at integer multiples of two fundamental conductance values, due to different molecule-electrode contact geometries.

The C-AFM break junction approach has been described in detail previously.[20] Octanedithiol molecules were first adsorbed onto a gold substrate by exposing the substrate to toluene containing 1 mM of octanedithiol. A Au-coated C-AFM probe was then brought into contact with the

* Corresponding authors. E-mail: Nongjian.Tao@asu.edu; diventra@physics.ucsd.edu.
[†] Arizona State University.
[‡] University of California.
[§] National Chiao Tung University.

10.1021/nl0608285 CCC: $33.50
Published on Web 05/23/2006

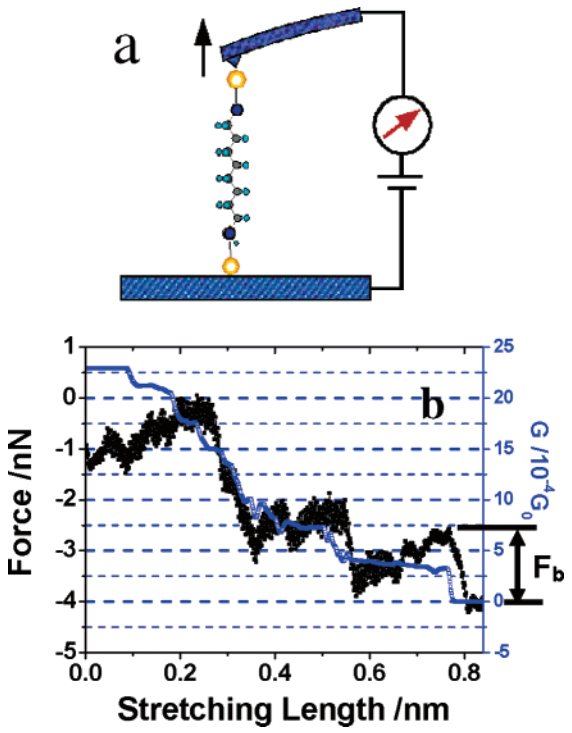

Figure 1. (a) Measurement of breakdown force of a molecule (1,8′-octanedithiol) covalently bound to two metal electrodes. (b) Simultaneously measured conductance (blue) and force (black) during the breakdown of a gold−octanedithiol−gold junction. The loading rate of the force applied to the AFM probe to break the bond is 803 nN/s, and the applied bias voltage is 0.1 V.

adsorbed molecules during which molecules may bridge between the AFM probe and the substrate via Au−thiolate bonds and form a multimolecule junction. This was followed by pulling the AFM probe away from the substrate, which resulted in a sequential breakdown of individual molecules from contacting the electrodes. When the last molecule was broken, the process was repeated so that we could perform a large number of measurements for statistical analysis. The measurements were performed in toluene in order to minimize the long-range attractions between the probe and the substrate and also possible contaminations.

We used monolithic silicon AFM probes (Budgetsensors-Tap300), which were coated with 50 nm Au (99.999%) in an ion beam coater (Gatan, Model 151). The spring constants of the probes were ∼33 N/m. The sample cell was made of Teflon cell, which was cleaned by boiling it in Piranha (98% H_2SO_4/30% H_2O_2 = 3:1, V/V) and then cleaned thoroughly by boiling in 18 MΩ Milli-Q-water (Nanopore system fed with campus distilled water) three times, followed by drying with N_2. (Caution: Piranha reacts violently with most organic materials, and must be handled with extreme care.) Gold substrates were prepared by evaporating 100−130 nm Au (99.999%) on freshly cleaved mica surfaces in the ion beam coater. Before experiment, an Au substrate was annealed with a H_2 flame and immediately immersed with toluene containing 1 mM of octanedithiol in the sample cell.

Figure 1b shows simultaneously recorded conductance and force curves obtained during the breakdown of the molecular junction. The conductance curve shows a series of steps due to the breakdown of the individual molecules. A conductance histogram constructed with ∼500 individual measurements reveals peaks with finite widths. The finite widths reflect a rather broad distribution of the conductance arising from different bonding geometries or atomic-scale configurations at the molecule−electrode contacts, and the peak positions are used to determine the conductance of the most probable configuration (Figure 2a). One set of conductance peaks are located at integer multiples of $\sim 2.6 \times 10^{-4}$ G_0 (high conductance, HC) where $G_0 = 2e^2/h \approx 77$ μS, where e is the electron charge and h is Planck's constant. Another set consists of peaks at $\sim 0.5 \times 10^{-4}$ G_0 (low conductance, LC, not shown here). These results are in good agreement with the previous STM-break junction results.[19] The conductance values are found to be independent of the loading rate within the entire rate range (Figure 2b). We have also determined the conductance as a function of bias voltage (V_{bias}) (Figure 3a). The conductance is independent of the bias below 0.5 V but increases with the bias above 0.5 V.

While the conductance decreases in discrete steps as one pulls the AFM tip away from the substrate, the corresponding force decreases like sawtooth waves (Figure 1b). Each discrete conductance jump is accompanied by an abrupt decrease in the force, which is called as breakdown force (F_b) due to the breakdown of a molecule from contacting with the electrodes.[20,21] The histogram of F_b corresponding to the conductance jump from the step located at $\sim 2.6 \times 10^{-4}$ G_0 (as marked in Figure 1b) constructed from ∼500 curves also reveals pronounced peaks with finite widths (Figure 2c). Similar to the conductance histograms shown in Figure 2a, the broad distribution of the breakdown force reflects different molecule−electrode contact configurations, and the peak position gives the most probable force (F^*) required to break an octanedithiol junction. However, unlike the conductance, which is independent of the loading rate, the breakdown force increases logarithmically with the loading rate below 800 nN/s. Above 800 nN/s, the force becomes independent of the loading rate (Figure 2d). This behavior is described well by the bond-breaking thermodynamic theory[22,23] and can be understood based on the following considerations. A chemical bond has a finite probability to break down spontaneously due to thermal fluctuations, and the probability of such a spontaneous breakdown process increases with time. So at a finite temperature, the required force to break the bond increases with the pulling or loading rate. At a very high loading rate (r_F > 800 nN/s in the octanedithiol system), the contribution from the thermal fluctuations diminishes and leads to the so-called adiabatic regime, in which the breakdown force becomes independent of the loading rate to overcome the dissociation energy barrier.

The most probable breakdown force determined in the adiabatic regime is ∼1.6 nN by fitting the force histogram with a Gaussian distribution. The error in the peak position is about 0.01 nN and standard deviation is 0.1−0.26 nN. The latter describes the distribution of the different molecule−electrode contact configurations.[21] We have also measured the breakdown force for Au−Au under the same condition

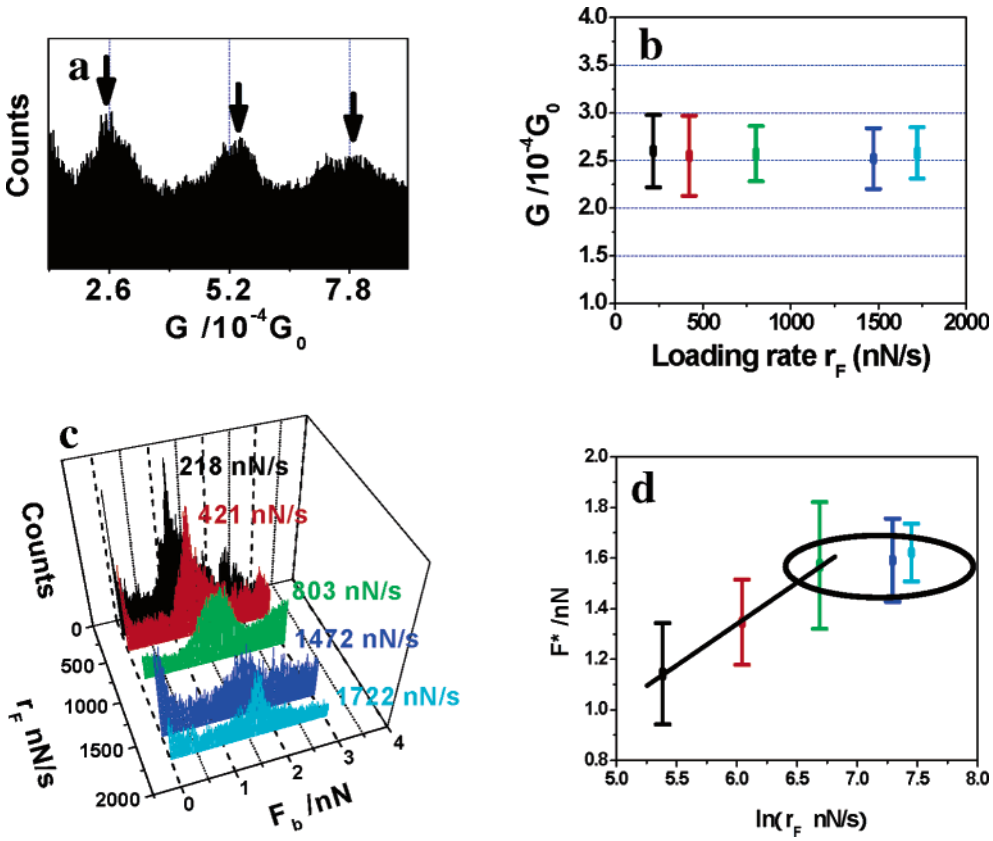

Figure 2. (a) Typical conductance histogram of octanedithiol obtained from ~500 individual measurements (loading rate 218 nN/s and bias 0.1 V). (b) Conductance of octanedithiol as a function of the loading rate (bias 0.1 V). We extracted the conductance value and error bar (the half-height of each data point in the plot) by fitting the histogram peaks with a Gaussian function. The standard deviations estimated from the Gaussian fitting are marked as error bars in the plot. (c) Breakdown force histograms, corresponding to the conductance jump from $\sim 2.6 \times 10^{-4}\ G_0$ (HC), are constructed from ~500 individual force curves at each loading rate (bias 0.1 V). (d) Average breakdown force (F^*) determined from the peak positions of the histograms in c as a function of logarithmic of the loading rate. Like the conductance, the average breakdown force and the error bars as the sizes of data points are determined from the Gaussian fitting. The standard deviations estimated from the Gaussian fitting are marked as error bars in the plot. The black line is a fit using eq 1, and the black circle marks the adiabatic regime.

and found a similar value. This result is consistent with low-temperature (4 K) measurements by Agrait et al.[24] On the basis of these observations, we can conclude that unless the S−Au bond strength coincides with the Au−Au bond strength, the breakdown of the octanedithiol junction most likely occurs at the Au−Au bond. This is supported by the observation of Au atoms attached to thiol molecules stripped off from a Au electrode.

In the logarithmically linear regime, the most probable breakdown force (F^*) is given by[23]

$$F^* = \frac{k_B T_{eff}}{x_\beta} \ln\left(\frac{t_{off}\, x_\beta}{k_B T_{eff}}\right) + \frac{k_B T_{eff}}{x_\beta} \ln r_F \qquad (1)$$

where k_B is Boltzmann's constant, T_{eff} is the effective temperature of the molecule-electrode contact, x_β is the average thermal bond length along the pulling direction until breaking, r_F is the force loading rate, and t_{off} is the lifetime of the bond. By fitting the experimental F^* versus ln r_F (Figure 2d) with eq 1, we have found that $t_{off} \approx 0.05$ s and $x_\beta \approx 0.013$ nm at a small bias (0.1 V), assuming that T_{eff} is equal to the room temperature (300 K) at the small bias. In the small bias limit, t_{off} can be expressed by

$$t_{off} = t_D \exp\left(\frac{E_b}{k_B T_{eff}}\right) \qquad (2)$$

where t_D is the diffusion relaxation time and E_b is the dissociation activation energy. E_b can be determined directly from the force versus stretching distance curves in the adiabatic regime ($r_F > 800$ nN/s), like the one shown in Figure 1b, using $E_b = {}^1/_2 F_b L$, where L is the extension distance over which the bond can be stretched before breakdown. We found the most probable $E_b^* \approx 0.66$ eV from the Gaussian fitting of the E_b histogram constructed in the adiabatic loading regime. Using the E_b^* value, together with $t_{off} \approx 0.05$ s, we determined t_D to be $\sim 3.5 \times 10^{-13}$ s at room temperature ($T_{eff} \sim 300$ K). Both E_b^* and t_D extracted from our experimental data are in good agreement with the theoretical values for Au−Au determined in refs 4, 6, and 25, which supports the fact that the breakdown of the octanedithiol junction most likely occurs at the Au−Au bond.

We have measured the most probable breakdown force, F^*, as a function of V_{bias} and found the force decreases with

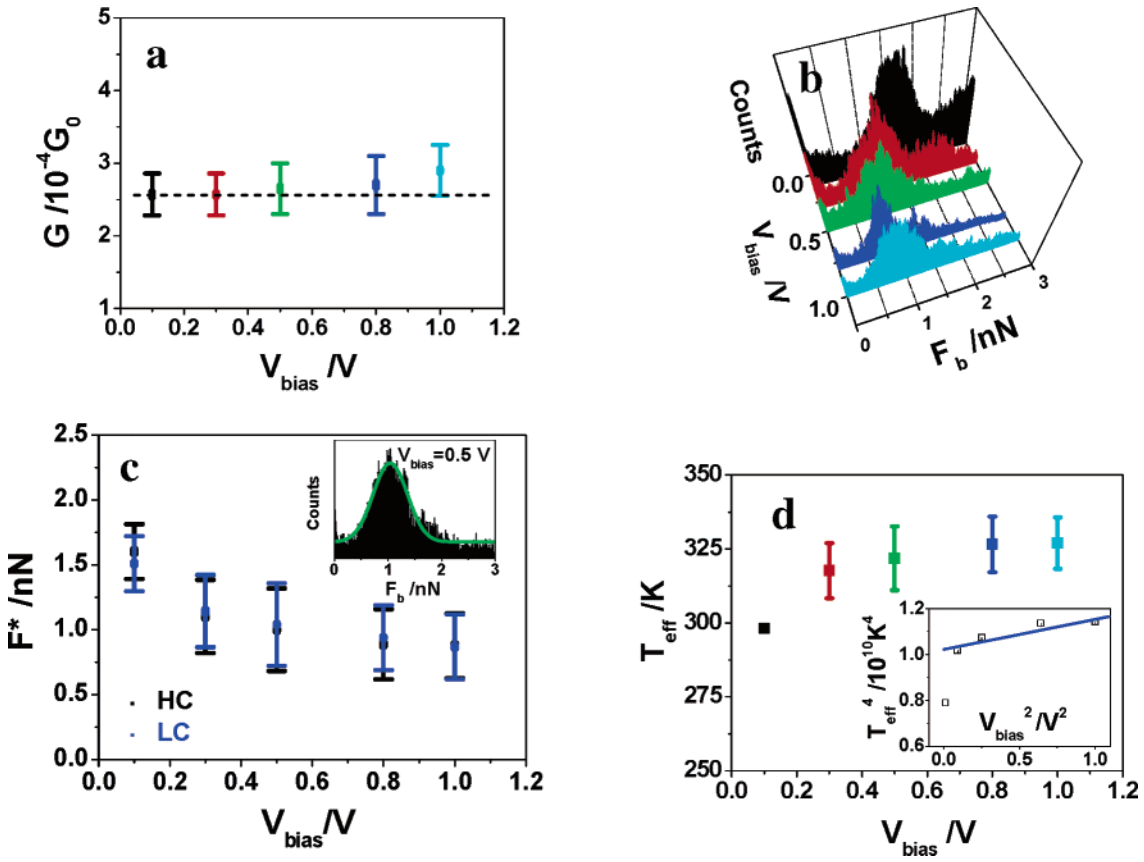

Figure 3. (a) Conductance of octanedithiol as a function of bias (loading rate 803 nN/s). The standard deviations estimated from the Gaussian fitting are marked as error bars in the plot. (b) Breakdown force histograms corresponding to the conductance jump from ~2.6 × 10^{-4} G_0 (HC) at various bias voltages (loading rate 803 nN/s). (c) Average breakdown force, F^*, vs bias voltage (loading rate 803 nN/s). Note that F^* in blue and black corresponds to the conductance jump from ~0.5 × 10^{-4} G_0 (LC) and ~2.6 × 10^{-4} G_0 (HC), respectively. The standard deviations estimated from the Gaussian fitting (inset) are marked as error bars in the plot. (d) Local temperature of octanedithiol, extracted from F^* corresponding to the conductance jump from ~2.6 × 10^{-4} G_0 (HC) at loading rate 803 nN/s, as a function of the bias and, inset, its fourth-power dependence on the square of the bias. The blue line in the inset of d is the best fit of the data using eq 4. Sizes of data points present error bars due to the uncertainty in peak positions estimated by the Gaussian fitting.

bias (Figure 3b and c). As we have mentioned earlier, there are two fundamental conductance values for octanedithiol bound to Au electrodes due to different molecule−electrode binding geometries. However, the breakdown forces of the two are not distinguishable within the experimental uncertainty (Figure 3c). There are two possible mechanisms that can cause the observed decrease in the breakdown force. One is current-induced forces, which may reduce the dissociation energy barrier and thus a smaller breakdown force.[4,26,27] This effect can be taken into account by modifying eq 2 into

$$t_{\text{off}} = t_{\text{D}} \exp\left(\frac{E_{\text{b}} - \alpha V_{\text{bias}}}{k_{\text{B}} T_{\text{eff}}}\right) \qquad (3)$$

where α is the electromigration coefficient describing the current-induced force, and T_{eff} is the effective temperature due to local heating effect. The electromigration coefficient, α, approximately equals the current-induced force at V_{bias} = 1 V multiplied by the stretching length at which the bond breaks. For a quantum point contact consisting of a chain of metal atoms between two bulk electrodes, α is found to be ~0.1 eV/V.[4,6,7] Current-induced forces arise as a result of charge redistribution around the atoms and are roughly proportional to the magnitude of the current.[4,26,27] Because the current in octanedithiol junctions is 4 orders of magnitude smaller than that of atomic point contacts, α should be much smaller than 0.1 eV/V, and the contribution of the current-induced force should thus have a negligible effect on lowering the activation energy barrier height (~0.66 eV) for the bias range studied here. We have confirmed this hypothesis by performing first-principles calculations (similar to the ones described in refs 3 and 27) on alkanedithiols of different lengths. We estimate α = 0.07 exp(−n) eV/V where n is the number of C atoms in the alkane chain. For octanedithiol (n = 8) we therefore find α to be of the order of 10^{-5} eV/V, which supports the conclusion that current-induced forces are very small for this molecule in this bias range.[27]

The second possible mechanism for the observed decrease in the breakdown force with the bias is the local heating effect we have discussed above, which increases the temperature of the molecule−electrode contact.[5,27] The dependence of the breakdown force on the local temperature is given by eq 1. At a given loading rate (803 nN/s), we have extracted T_{eff} using eqs 1 and 2 together with E_{b}*, x_β, and t_{D} given above, as a function of bias voltage (Figure 3d). We see from this figure that the increase in the local temperature

due to current-induced heating is about 30 K above the ambient room temperature at a bias of 1 V.

If we assume a bulk lattice heat conduction law, then the temperature, T_{eff}, can be approximately related to V_{bias} according to[4,5,9,25]

$$T_{\text{eff}}^4 = T_0^4 + \gamma^4 V_{\text{bias}}^2 \quad (4)$$

where T_0 is the ambient temperature and γ is a constant that describes the magnitude of the local heating effect. Our data can be roughly fit with eq 4 with $\gamma \approx 190$ K/V$^{1/2}$. From our first-principles calculations, we determine $\gamma = 375 \exp(-0.19n)$ K/V$^{1/2}$ for different numbers (n) of C atoms in the chain. For octanedithiol, we therefore find $\gamma \approx 82$ K/V$^{1/2}$. Given that the details of the bonds at the molecule−electrode interface in the experiment are not known, this level of agreement between the experimental data and theoretical estimate can be considered good.

We note that the error bars in the plot (Figure 3d) are due to the distribution of different contact configurations, and the errors due to the uncertainty in the peak positions of the force histograms are given by the sizes of the data points. Even if we consider the wide distribution in the extracted temperature, then the fit to eq 4 is good only at larger biases (see the inset of Figure 3d). A possible reason for this deviation is that phonon modes localized at the molecule−metal contact, which are weakly bound to the bulk electrodes, may be present at low energies. For these modes, a bulk law for heat conduction is not necessarily appropriate, and deviations from eq 4 are expected.[5,25]

In summary, we have studied local heating effects in single molecules (octanedithiol) covalently bound to two electrodes by measuring the average force needed to break the molecule−electrode bond. At a bias voltage of 1 V, the temperature is raised ∼30 K above the ambient room temperature. Above this bias, the molecule junction becomes increasingly unstable. The results are in good agreement with theoretical calculations of local heating effects in this system.

Acknowledgment. We thank Peter Bennett and Mark van Schilfgaarde for valuable discussions and NSF (ECS0304682) (Z.H.) and DOE (DE-FG03-01ER45943) (B.X.) for financial support. M.D. and Y.C. acknowledge support from NSF Grant no. DMR-01-33075 and Taiwan National Science Council Grant no. NSC 95-2112-M-009-024.

References

(1) Aviram, A.; Ratner, M. *Chem. Phys. Lett.* **1974**, *29*, 277.
(2) Carroll, R. L.; Gorman, C. B. *Angew Chem., Int. Ed.* **2002**, *41*, 4379.
(3) (a) Nitzan, A.; Ratner, M. A. *Science* **2003**, *300*, 1384. (b) See also Introduction to *Nanoscale Science and Technology*; Di Ventra, M., Evoy, S., Heflin, J. R., Eds.; Springer: New York, 2004.
(4) Todorov, T. N. Hoekstra, J.; Sutton, A. P. *Phys. Rev. Lett.* **2001**, *86*, 3606.
(5) (a) Chen, Y.-C.; Zwolak, M.; Di Ventra, M. *Nano Lett.* **2003**, *3*, 1691. (b) Chen, Y.-C.; Zwolak, M.; Di Ventra, M. *Nano Lett.* **2004**, *4*, 1709. (c) Chen, Y.-C.; Zwolak, M.; Di Ventra, M. *Nano Lett.* **2005**, *5*, 621.
(6) Smit, R. H. M.; Untiedt, C.; van Ruitenbeek, J. M. *Nanotechnology* **2004**, *15*, S472.
(7) Tsutsui, M.; Taninouchi, Y.-k.; Kurokawa, S.; Sakai, A. *Jpn. J. Appl. Phys., Part 1* **2005**, *44*, 5188.
(8) Segal, D.; Nitzan, A. *J. Chem. Phys.* **2002**, *117*, 3915.
(9) Chen, Y.-C.; Di Ventra, M. *Phys. Rev. Lett.* **2005**, *95*, 166802.
(10) York, R. L.; Nguyen, P. T.; Slowinski, K. *J. Am. Chem. Soc.* **2003**, *125*, 5948.
(11) Holmlin, R. E.; Haag, R.; Chabinyc, M. L.; Ismagilov, R. F.; Cohen, A. E.; Terfort, A.; Rampi, M. A.; Whitesides, G. M. *J. Am. Chem. Soc.* **2001**, *123*, 5075.
(12) Slowinski, K.; Chamberlain, R. V.; Miller, C. J.; Majda, M. *J. Am. Chem. Soc.* **1997**, *119*, 11910.
(13) Wold, D. J.; Frisbie, C. D. *J. Am. Chem. Soc.* **2001**, *123*, 5549.
(14) Chidsey, C. E. D. *Science* **1991**, *251*, 919.
(15) Wang, W.; Lee, T.; Reed, M. A. *Phys. Rev. B* **2003**, *68*, 035416/1.
(16) Xu, B. Q.; Tao, N. J. *Science* **2003**, *301*, 1221.
(17) Cui, X. D.; Primak, A.; Zarate, X.; Tomfohr, J.; Sankey, O. F.; Moore, A. L.; Moore, T. A.; Gust, D.; Harris, G.; Lindsay, S. M. *Science* **2001**, *294*, 571.
(18) He, J.; Sankey, O.; Lee, M.; Tao, N.; Li, X.; Lindsay, S. *Faraday Discussions* **2006**, *131*, 145.
(19) Li, X.; He, J.; Hihath, J.; Xu, B.; Lindsay, S. M.; Tao, N. *J. Am. Chem. Soc.* **2006**, *128*, 2135.
(20) Xu, B. Q.; Xiao, X. Y.; Tao, N. J. *J. Am. Chem. Soc.* **2003**, *125*, 16164.
(21) Velez, P.; Dassie, S. A.; Leiva, E. P. M. *Phys. Rev. Lett.* **2005**, *95*, 045503/1.
(22) Bell, G. I. *Science* **1978**, *200*, 618.
(23) Evans, E. *Annu. Rev. Biophys. Biomol. Struct.* **2001**, *30*, 105.
(24) Rubio, G.; Agrait, N. Vieira, S. *Phys. Rev. Lett.* **1996**, *76*, 2302.
(25) Todorov, T. N. *Philos. Mag. B* **1998**, *77*, 965.
(26) Di Ventra, M.; Pantelides, S. T.; Lang, N. D. *Phys. Rev. Lett.* **2002**, *88*, 046801.
(27) Yang, Z.; Chshiev, M.; Zwolak, M.; Chen, Y.-C.; Di Ventra, M. *Phys. Rev. B* **2005**, *71*, 041402.

NL0608285